Received: 2 July 2024 | Revised: 26 August 2024 | Accepted: 2 September 2024

DOI: 10.1002/pc.29064

RESEARCH ARTICLE

Polymer COMPOSITES WILEY

Effect of geometric configurations and curvature angle of corrugated sandwich structures on impact behavior

Ilyas Bozkurt

Department of Mechanical Engineering, Architecture and Engineering Faculty, Mus Alparslan University, Mus, Turkey

Correspondence
Ilyas Bozkurt, Department of Mechanical Engineering, Architecture and Engineering Faculty, Mus Alparslan University, Mus 49250, Turkey.
Email: i.bozkurt@alparslan.edu.tr

Abstract

The aim of this study is to numerically investigate the low-velocity impact behavior of carbon fiber reinforced orthogonal woven fabric composite sandwich structures with five different geometric configurations and four different curve angles. Low velocity impact simulations were performed in *LS DYNA* finite element program to investigate the effects of core configuration and curve angle on peak contact force, energy absorption efficiency and damage mode. A progressive damage analysis based on the combination of the Hashin damage criterion and the *Cohesive Zone Model (CZM)* with *bilinear traction-separation law* was performed using the *MAT-54 (ENHANCED_COMPOSITE_DAMAGE)* material model. Among the five different cores, Trapezoidal core has the highest peak force average of 2.9 kN while Triangular core sandwich structure has the lowest with 1.23 kN. Absorbed energy efficiency average was highest for rectangular core with 0.95 and lowest for sinusoidal core with 0.69. The specific absorbed energy value was highest for Triangular core with 0.312 J/g and lowest for Sinusoidal core with 0.178 J/g. The damage area on the structure increased with increasing curve angle. It was determined that the core structure and curve angle is an effective parameter on peak force and energy absorption efficiency.

Highlights

- Impact behavior of sandwich composite structures was examined.
- The effects of core type and curve angles on peak force, energy absorption efficiency and specific absorption energy were investigated.
- Specific absorption energy rates were compared with studies in the literature.

KEYWORDS

cohesive zone model (CZM), curved sandwich composite, finite element method, low velocity impact test, progressive damage analysis

1 | INTRODUCTION

Composite materials are used in many sectors, especially in the defense industry, due to their high strength-to-weight ratio and excellent energy absorption capacity.[1] Sandwich composite structures stand out especially in parts and components where energy absorption is required. Sandwich structures are a type of composite consisting of core structures with different shapes and structures between the upper and lower facesheet. With the development of manufacturing technology and production techniques, it has become possible to produce composite structures in many different structures and configurations.[2] They can be manufactured from different materials according to the sector to be used and the component at the application point. When the studies on composite structures are examined, it is seen that the interest in curved surfaces has increased in the last decade. It is seen that curved surface structures are used in aircraft noses, wing and body structures in the aviation industry, military vehicles in the defense industry, bullet-proof clothing, ship structures and motor boats. Due to the superior properties of sandwich composite structures, they can be used in many different areas and components and can be exposed to very different loading conditions. However, sandwich composites are susceptible to impact damage due to the complexity of their micro-mechanical structures and energy absorption system under load.[3] The invisible damages in the structure directly affect the stiffness and lifetime of the structure. Therefore, determining the impact behavior of these structures and obtaining detailed information about the damage mechanisms is of great importance for safety.[4]

The main purpose of using corrugated structures is to reduce the total weight of the system. Especially in metal structures, when corrugated structure is used instead of the whole volume, the total weight is significantly reduced.[5] This is very important in the aviation industry where weight is an important influence on fuel consumption. In recent years, with the improvement of the mechanical performance of composite structures, the use of composites in applications requiring mechanical strength is increasing. It is seen that curved composite structures have entered our lives from bicycle body to vehicle and aircraft parts.

Many studies have been conducted to improve the mechanical performance of corrugated sandwich composite structures.[6–12] Cao et al.[13] experimentally investigated the impact behavior of multilayer corrugated sandwiches. They also compared the experimental results on the velocity sensitivity of single-layer and multilayer sandwiches. Kilicaslan et al.[14] experimentally and numerically investigated the impact behavior of interlayer sandwich panels with corrugated aluminum core and aluminum alloy surfaces using spherical and flat striking tips. Yu et al.[15] investigated the low-velocity impact response of hollow extruded aluminum alloy corrugated sandwich beams used in the bodies of high-speed trains. The damage mechanism map of the corrugated sandwich beam under low-speed impact was obtained by theoretical analysis, which was verified by experimental and finite element simulation results. He et al.,[9] experimentally and numerically investigated the low-velocity impact response and post-impact bending behavior of hybrid sandwich structures composed of carbon fiber reinforced polymer (CFRP) surface layers and aluminum alloy corrugated cores. Li et al.[16] investigated the performance and energy absorption of Kirigami corrugated core sandwich structures under dynamic crushing through pendulum impact tests. Acanfora et al.[17] conducted experimental and numerical investigations to determine the mechanical behavior of lightweight sandwich composite structures with polypropylene core and carbon fiber reinforced polymer facesheets in shock absorption applications. The investigated sandwich structures used a Designed for Additive Manufacturing (DfAM) core to maximize their performance in terms of energy-to-weight ratio and damping of impact loads. Garofano et al.[18] performed numerical simulations to determine the stresses and accelerations on the occupants during an aircraft collision. They numerically studied the side impact of an airline passenger with a World SID-based dummy positioned in the window-side seat of an aluminum commercial aircraft fuselage. The numerical results were cross-matched with literature experimental data. Rong et al.[19] numerically investigated the impact and crushing performance of geometric configurations of corrugated cores. Zhao et al.[20] investigated the behavior of glass fiber reinforced double corrugated sandwich composite structures under low velocity impact. Shui Yang et al.[21] investigated the impact strength and damage mechanisms of carbon fiber composite circular corrugated sandwich cylindrical panel produced by hot press molding method. They used validated finite element analysis (FEA) models based on *Hashin failure criteria* to investigate the effects of relative density, impact energy and impact location on impact responses.

Cheng et al.[22] experimentally and numerically investigated the low-velocity impact behavior of U-type corrugated sandwich panels. Boonkong et al.[23] experimentally and numerically investigated the low-velocity impact behavior, energy absorption performance and damage mechanisms of lightweight aluminum sandwich panels with curvilinear aluminum alloy cores. Yellur et al.[24] experimentally and numerically examined the effects of upper and lower facesheet thicknesses on impact

behavior in polypropylene honeycomb sandwich structures. They used the *LS-DYNA* finite element model for numerical analysis. Susainathan et al.[25] numerically investigated the impact behavior of innovative wood-based sandwich structures with plywood cores and coatings made of aluminum or fiber-reinforced polymer (carbon, glass or flax composite coatings). Numerical models were created with *LS DYNA*. Shirbhate et al.[26] examined the explosion response of a hexagonal honeycomb sandwich structure with holes along the cell height of the core compared to conventional honeycomb cores. They performed detailed numerical analysis to accurately reproduce the deformation process by finite element analysis using the open *LS-DYNA* software.

Many different tests and laboratories are needed to produce composite structures, which have a wide range of applications, to test the produced specimens and to determine their mechanical performances.[27] The limited and high cost of the materials needed in the production processes and the trial-and-error testing of the produced specimens using high-cost testing equipment limit the researchers.[28] Due to these high costs, researchers have carried out the production and testing stages with the help of finite element programs.[29] However, although the accuracy of finite element analysis has increased with the advances in finite element technology, the accuracy rate decreases when these analysis results are not supported by experimental work. In order to overcome this problem, the researchers created a numerical model with reference to experimental studies that were previously conducted with high costs and difficulties.[30–32] Setoodeh et al.[33] used a three-dimensional elasticity-based FEM approach coupled with layered laminated plate theory to perform low-velocity impact analysis of fiber-reinforced laminated composite plates. Khalili et al.[34] investigated the dynamic and quasi-static impact behavior of cylindrical structures using finite element method. The effects of cylindrical composite plate and shell structures and various edge/thickness ratios were investigated. In order to support the finite element results, the results of previous composite plate, curved composite laminate, composite thick cylinder and composite thin cylinder experiments in the literature were taken as reference.

In this study, unlike the literature, the low-velocity impact behavior of carbon fiber reinforced orthogonal woven fabric composite sandwich structures with five different geometric configurations (Trapezoidal, Rectangular, Arc-shaped, Triangular and Sinusoidal) and four different curvature angles (0°, 90°, 120°, 150°) were numerically investigated. A previous experimental study is taken as a reference to support the numerical model. In order to investigate the effects of core structure and curve angle on peak contact force, impact energy absorption and damage mode, low velocity impact tests were performed in *LS DYNA* finite element program. At the end of the study, the specific energy absorption values were compared with the studies in the literature.

2 | EXPERIMENTAL STUDY

It is important that the numerical model to be used in the study is supported by an experimental study in order for the analysis to give accurate results. Therefore, in this study, firstly, the numerical model was created by taking the experimental study of Reference 21, the numerical model was created with reference to the experimental study.

In the study, hot press molding method was used to produce carbon fiber composite circular corrugated sandwich cylindrical panels using carbon fiber reinforced orthogonal woven fabric composite. The macro mechanical properties of the material listed in Table 1 were tested using Instron 5505 test rig in accordance with ASTM D695-96[35] and ISO 527-4 guidelines.[36] The dimensions given here correspond to $d = 11\,\text{mm}$, $H = 160\,\text{mm}$, $f_a = 5.91\,\text{mm}$, $\alpha = 120^\circ$ ve $\theta_a = 53.5^\circ$. The test setup for the impact test is given in Figure 1.

In low velocity impact tests, many graphs and data about the mechanical performance of the material are obtained. In these graphs and outputs, it is decided whether the material is suitable for the component or position to be used or not by comparing according to the standards. In the weight drop experimental test setup, these data are obtained by reading from the tip of the impactor. Along with the changes in the kinetic energy and velocity of the impactor, displacement graphs are extracted from its position. Equations (1)–(4) are used to obtain the changes in velocity, displacement and energy with respect to the impact timing of the impactor. Data on contact force, displacement and absorbed energy obtained from the tip of the impactor were evaluated.

$$v(t) = v_i + gt - \int_0^t \frac{F(t)}{m} d(t) \tag{1}$$

Here, t is the time of the first contact of the impactor to the specimen, which is $t = 0$; $v(t)$ is the velocity of the impactor at time t; v_i is the velocity of the impactor at time $t = 0$; and $F(t)$ is the impact contact force measured at time t.

$$\delta(t) = \delta_i + v_i t + \frac{gt^2}{2} - \int_0^t \left(\int_0^t \frac{F(t)}{m} dt \right) dt \tag{2}$$

TABLE 1 Dimensions and masses of corrugated core structures.

Cell name	Cell shape	Mass (gr)
Trapezoidal	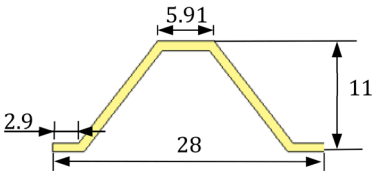	47.8
Rectangular	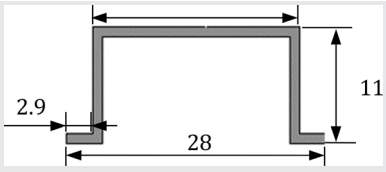	61.2
Arc-shaped	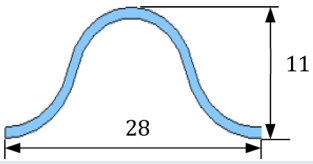	46.9
Triangular	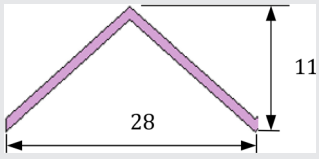	43.6
Sinusoidal	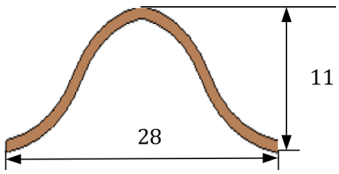	45.2

δ is the displacement of the impactor at time t, while δ_i is the displacement of the impactor from the reference point at time $t = 0$.

$$E_a(t) = \frac{m\left(v_i^2 - (v(t))^2\right)}{2} + mh\delta(t) \quad (3)$$

Here, $E_a(t)$ is the absorbed energy at time t, m is the weight impact, and g is the gravitational acceleration. To evaluate the weight efficiency of the energy absorption of a structure, the specific energy absorption (SEA) is generally used.

$$SEA = \frac{E_a}{m} \quad (4)$$

Here, m is the mass of the crash structure. Higher SEA values indicate better energy-absorbing efficiency of the structures.

3 | NUMERICAL STUDY

3.1 | Finite element model

Low velocity impact behavior of carbon fiber reinforced orthogonal woven fabric composite sandwich structures with different geometric configurations and curvature angles was investigated using *LS DYNA* finite element program.[37]

The solution methodology of the program includes material cards that provide damage models based on the *continuous damage mechanism* (CDM).[38] By using models based on CDM, it is possible to see structural damage in a progressive manner. Impact tests were performed numerically for all specimens used in this study with dimensions of 140 × 160 mm. The drawings of the sandwich structures formed by the combination of the core structure placed between the upper and lower surfaces were made in *Solidworks* program. In the study,

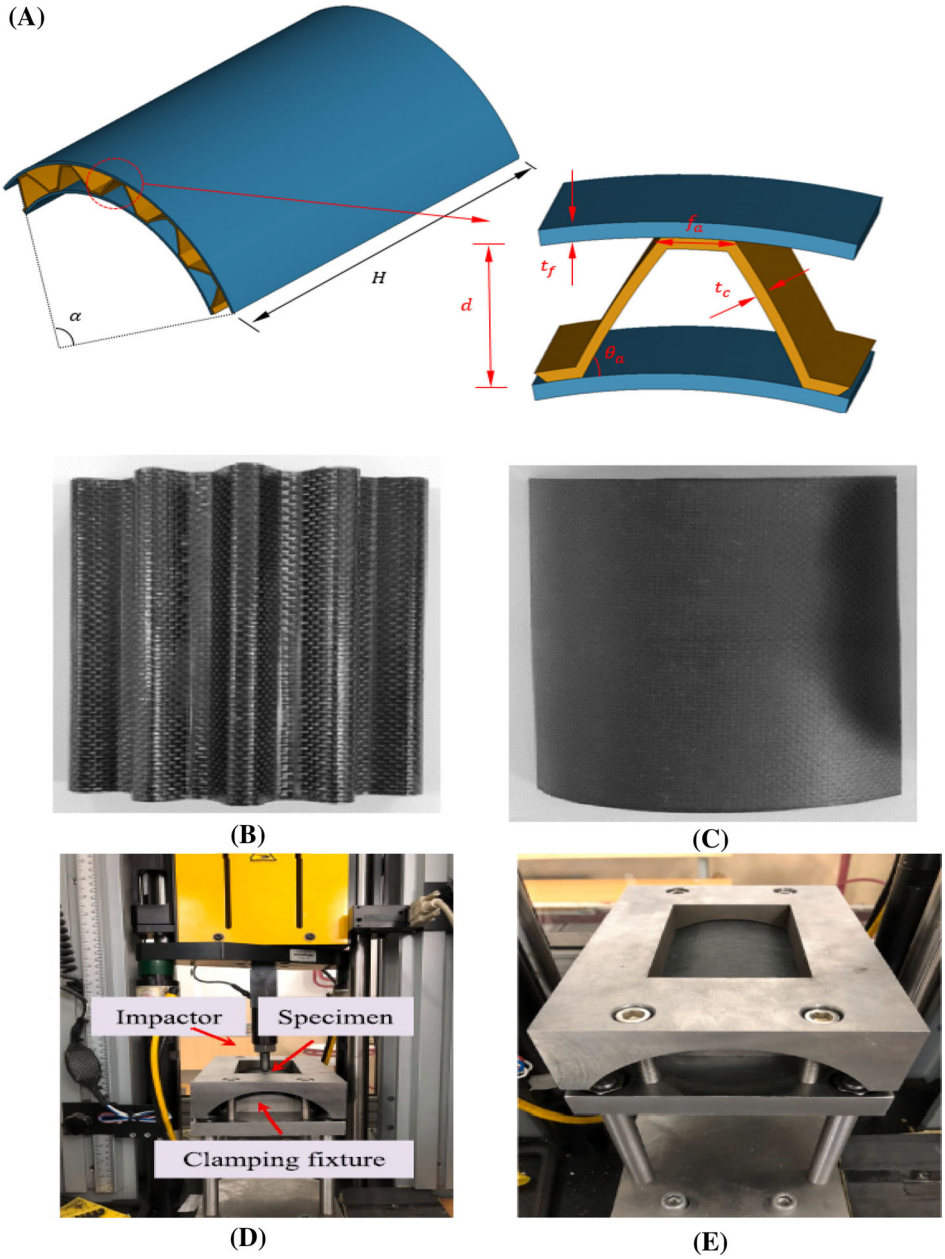

FIGURE 1 (A) Dimensions of the test specimen, (B) Corrugated core, (C) face sheet, (D) impact test apparatus, (E) specimen and clamping apparatus for impact test.[21]

8-node brick solid element (*ELFORM1*) was used for all elements. Mesh convergence study was performed and it was seen that the most compatible mesh structure with the experimental study was 2 × 2 mm. Moreover, when criteria such as analysis time and proximity to the experimental study were evaluated, this mesh structure was determined to be the most suitable. Figure 2 shows the FE model used in the study and different corrugated core structures used in the research. The diameter of the hemispherical steel impactor is 12 mm, length is 36 mm and weight is 8.37 kg. The tests were carried out by setting the impactor to.

15 J impact energy. The direction of movement of the impactor is restricted for x and y directions. It is only allowed to move in the z direction. The upper and lower holders are considered completely fixed. That is, its movement is restricted for x, y and z directions. These boundary conditions are based on the experimental study. Because the results in FE analysis are appropriate and close to the experimental study depends on these boundary conditions. A total of 82,709 nodes and 54,784 solid elements were used in the modeling. The upper and lower holders were modeled with 11,668 nodes and 5312 solid elements.

CONTACT_AUTOMATIC_SURFACE_TO_SURFACE contact card was used to model the contact force between the sandwich composite and the impactor and to prevent the specimen from moving between the holders during impact. The static and dynamic friction coefficients were entered as 0.2 and 0.3 respectively.[27] The CONTACT

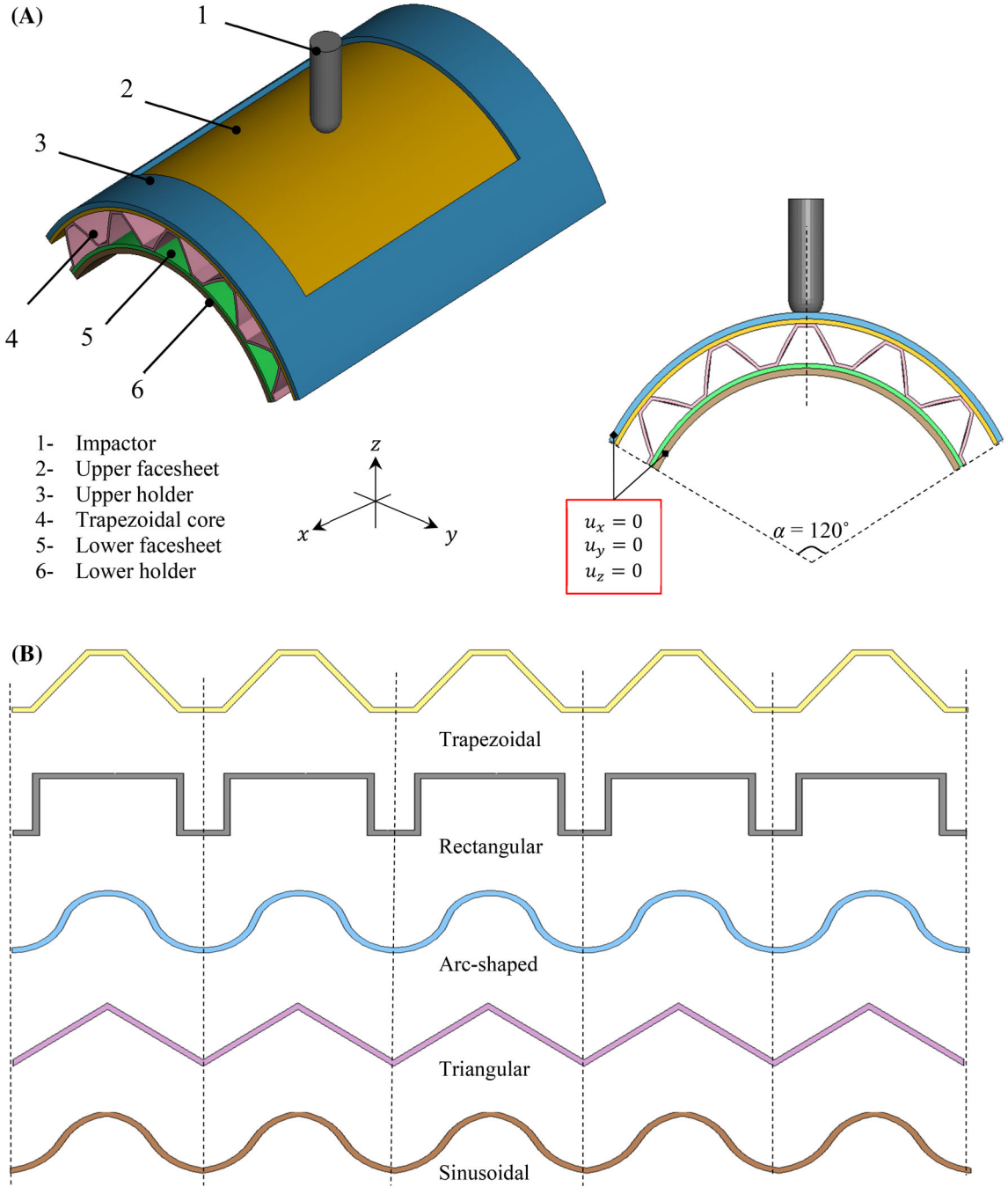

FIGURE 2 (A) FE models of the low velocity impact test, (B) Different corrugated core structures used in the research.

AUTOMATIC SINGLE SURFACE card was used to prevent all elements from interfering with each other due to the impact.

Five different (Trapezoidal, Rectangular, Arc-shaped, Triangular and Sinusoidal) corrugated core structures with different geometric configurations and curve angles were investigated in the study. Figure 2B shows the shapes of the Trapezoidal, Rectangular, Arc-shaped, Triangular and Sinusoidal core structures used in the study. Core dimensions and curve shapes of these structures are given in Tables 1 and 2 respectively. Their masses were found by calculating their volumes in FE. The thickness value and face sheet thickness of all specimens are 1 mm. The cell width and cell heights used in all structures are equal.

3.2 | Material models

There are many material models that describe composite materials in the LS-DYNA finite element program.

TABLE 2 Curve corrugated sandwich structures used in the study.

	$\alpha = 0^{\circ}$	$\alpha = 90^{\circ}$	$\alpha = 120^{\circ}$	$\alpha = 150^{\circ}$
Trapezoidal	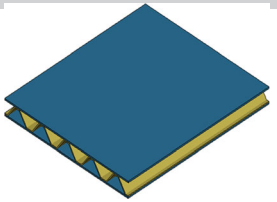	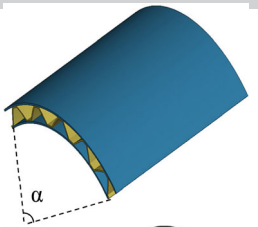	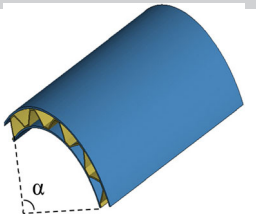	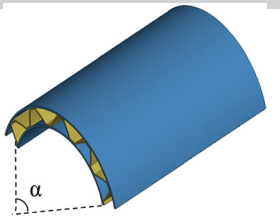
Rectangular	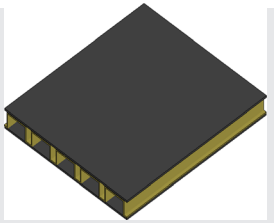	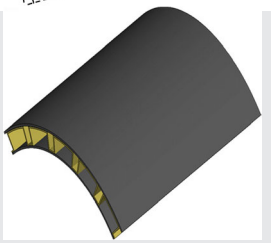	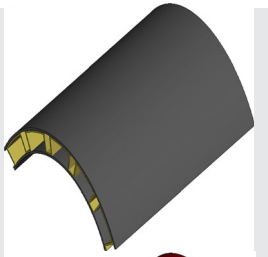	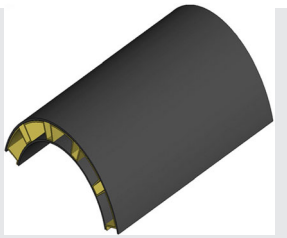
Arc-shaped	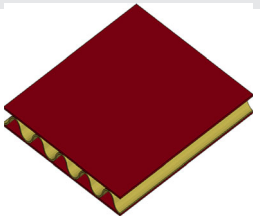	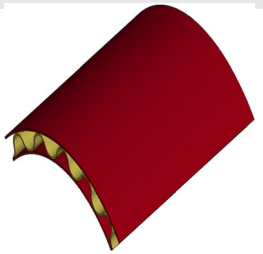	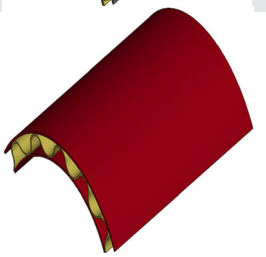	
Triangular	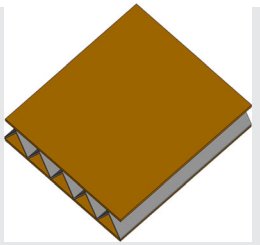	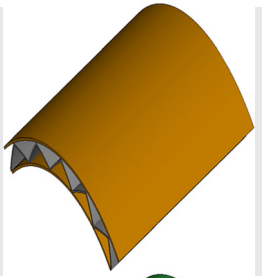	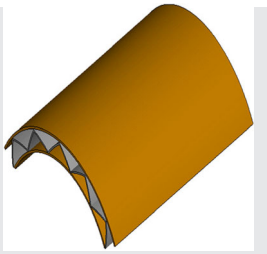	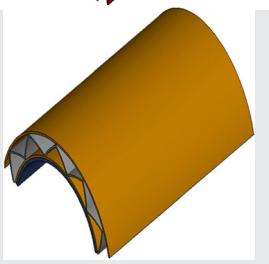
Sinusoidal	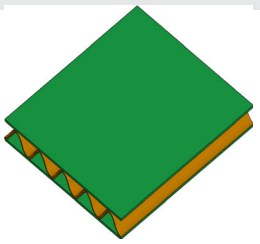	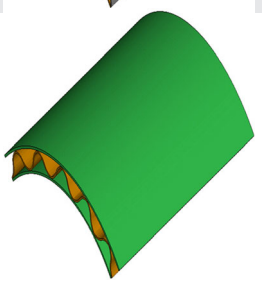	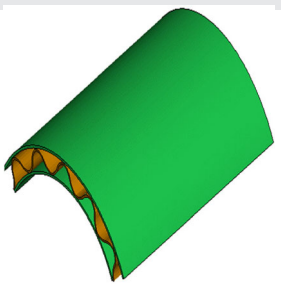	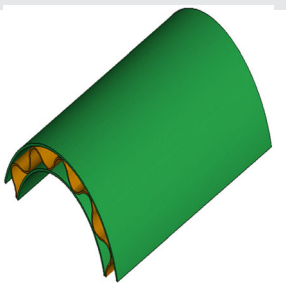

The choice of these models varies according to the intended use. MAT-54 material model was used in this study. In this material model, fiber damage, matrix damage and delamination behavior under impact loading can be determined based on the progressive damage principle. Hashin damage criteria[39] are applied with this material model. A total of 24 parameters are required to introduce the MAT-54 material model to the program. Details of these parameters are given in Tables 3, 4.

3.3 | Modeling of adhesive layer

In sandwich structures, the core structure and the upper and lower facesheets structures need to be bonded to each other. Different types of adhesives such as resin or Araldite 55 are used to ensure this bonding. These adhesives are applied to the contact points of the core and facesheet structures and adhesion is achieved by waiting for a certain period of time at room temperature. This adhesion is of great importance in absorbing the force coming to the upper facesheet in case of impact and distributing it homogeneously to other areas. Therefore, this adhesion and separation due to impact is based on some mechanical principles. In the literature, it is characterized as CZM with a *bilinear traction-separation law*. This law is based on the application of 3 independent parameters. The traction t_0, between the layers when the force is applied, the separation distance δ_0 when the damage starts and the G_C under this curve. After the impact occurs, the separation between the layers occurs according to this principle (Figure 3).

Adhesion here can be achieved in two ways. First, it can be achieved by defining a thin interfacial material between the top cover and the core in the middle. Or it can be achieved by using a bonding surface that performs the same function. Dogan et al.[40] found this method to be effective instead of using an intermediate material. In this study, The CONTACT_AUTOMATIC SURFACE TO SURFACE TIEBREAK contact board was used to bond the top and bottom cover to the core material in between. While adhesion is achieved here, separations occur based on the Bilinear traction-separation law. With this contact card, the nodes making contact in the beginning connect with each other according to the following criterion.

$$\left(\frac{|\sigma_n|}{NFLS}\right)^2 + \left(\frac{|\sigma_s|}{SFLS}\right)^2 \geq 1 \tag{5}$$

Here, while σ_n and σ_s are the current normal and shear stresses, *NFLS* and *SFLS* are respectively the interface and shear strength. When the condition of Equation (5) is met, interface node stress is decreased to zero and the connection between the nodes is released. The contact parameters for Araldite 2015, which was used as the adhesive material in this research, are provided in Table 5.

3.4 | MAT_54–55: Enhanced composite damage model

It is the most widely used material model in the analysis of composite structures. In the material model, it is assumed that the material is orthotropic and linear elastic in the absence of any damage. In this model, *MAT 54* damage criterion was proposed by *Chang* and *MAT 55* damage criterion was proposed by *Tsai-Wu*. This material model has the

TABLE 3 Mechanical parameters of the GFRP composite.[21]

Symbol	Property	Value	Unit
ρ	Density	1523	kg/m^3
E_a, E_b	Young modulus *a* and *b* direction	63	GPa
E_c	Young modulus in *c* direction	11	GPa
υ_{ab}	Poisson's ratio in *ab* plane	0.063	-
υ_{bc}	Poisson's ratio in *bc* plane	0.32	-
υ_{ca}	Poisson's ratio in *ca* plane	0.063	-
G_{ab}	Shear modulus in *ab* plane	4.2	GPa
G_{bc}	Shear modulus in *bc* plane	4.2	GPa
G_{ca}	Shear modulus in *ca* plane	4.2	GPa
S_{aT}	Tensile strength *a* direction	0.756	GPa
S_{aC}	Compressive strength *a* direction	0.557	GPa
S_{bT}	Tensile strength *b* direction	0.756	GPa
S_{bC}	Compressive strength *b* direction	0.557	GPa
S_{ab}	Shear strength in *ab* plane	0.118	GPa

same operating principle as the *MAT 22* model but additionally includes a compression damage mode. The Chang–Chang criterion (*MAT_54*) is given below;

Tensile fiber ($\sigma_{11} > 0$).

$$\left(\frac{\sigma_{11}}{S_1}\right)^2 + \overline{\tau} = 1 \tag{6}$$

TABLE 4 Failure parameters of the GFRP composite.

Symbol	Description	Unit
DFAILM	Transverse matrix failure strain experimental	0.0
DFAILS	Shear failure strain experimental	0.0
DFAILT	Tensile fiber failure strain experimental	0.0
DFAILC	Compressive fiber failure strain experimental	0.0
TFAIL	Timestep for element deletion computational	0.16
Alpha	Shear stress parameter damage dependent	0.0
Soft	Strength reduction factor damage dependent	0.7
FBRT	Reduction factor for X_t damage dependent	1
YCFAC	Reduction factor for X_c damage dependent	3
EFS	Efective failure strain computational	0.90

All moduli and Poisson's ratios are set to zero when the tensile fiber failure criteria are met, that is $E_1 = E_2 = G_{12} = \upsilon_{12} = \upsilon_{21} = 0$ All the stresses in the elements are reduced to zero, and the element layer has failed.

Failure mode for compressive fiber ($\sigma_{11} > 0$),

$$\left(\frac{\sigma_{11}}{S_{12}}\right)^2 = 1 \tag{7}$$

Failure mode for tensile matrix ($\sigma_{11} > 0$),

$$\left(\frac{\sigma_{22}}{S_2}\right)^2 + \overline{\tau} = 1 \tag{8}$$

Failure mode for compressive matrix.

$$\left(\frac{\sigma_{22}}{2S_{12}}\right)^2 + \left[\left(\frac{C_2}{2S_{12}}\right) - 1\right]\frac{\sigma_{22}}{C_2} + \overline{\tau} = 1 \tag{9}$$

where E_1 and E_2 are the longitudinal and transverse elastic moduli, respectively, G_{12} is the shear modulus, υ_{12} and υ_{21} are the in-plane Poisson's ratios.

TABLE 5 Cohesive parameters between core and face sheets interfaces.[41]

Contact tiebreak variable	Description	Value	Units
NFLS	Peak traction in normal direction	21.63×10^9	Pa
SFLS	Peak traction in tangential direction	17.9×10^9	Pa
PARAM	Exponent of mixed-mode criteria	1	-
ERATEN	Energy release rate for Mode I	430	N/m
ERATES	Energy release rate for Mode II	4700	N/m
CT2CN	Ratio of tangential stiffness to normal stiffness	1	-
CN	Normal stiffness	8080	Pa/m

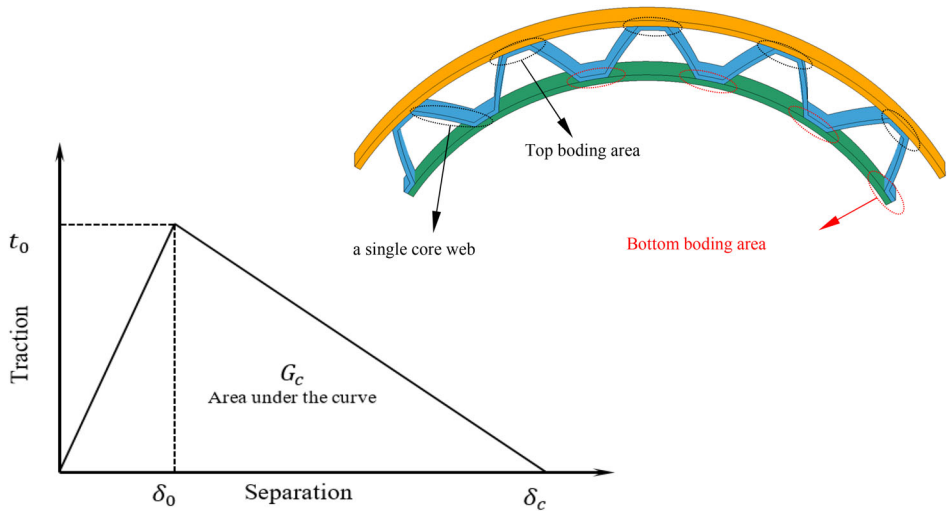

FIGURE 3 Bilinear traction-separation law.

4 | RESULTS AND DISCUSSION

The contact force-time and kinetic energy-time graphs obtained from low velocity impact of five different corrugated sanwich composite structures with different configurations and curve angles are given in Figure 4. The impactor energy was set to 15 J. When the contact force-time plot of Figure 4A is examined, it is seen that the result obtained with the FE model is close to the experimental study. The difference between the experimental and numerical results is 1.8% for peak force. It is seen that the contact force value increases with the effect of the impact.[42] After the force value reaches the peak value, it is

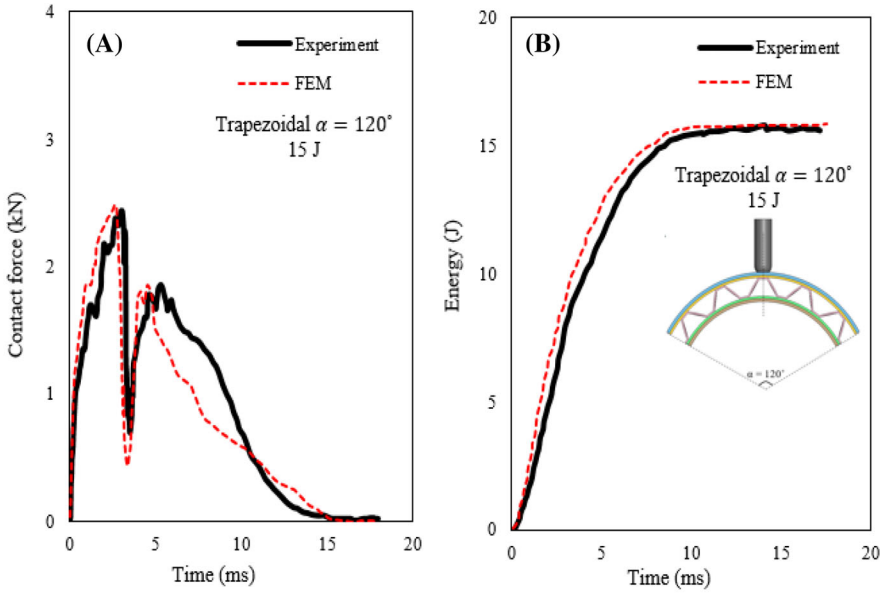

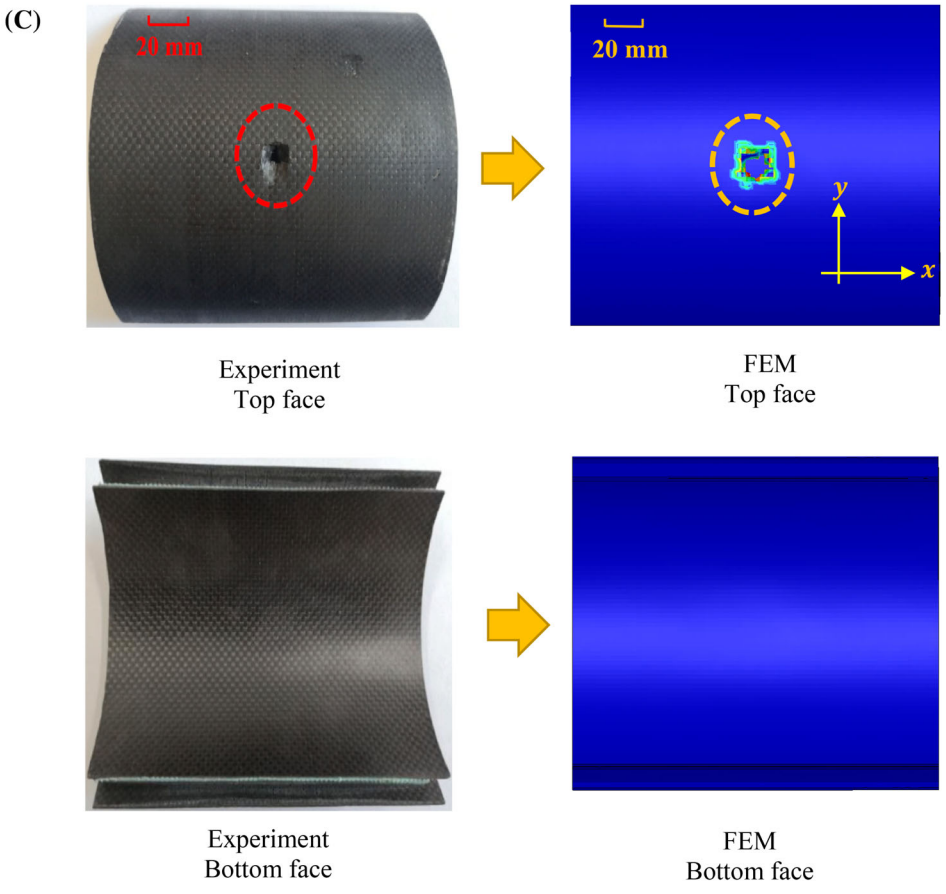

FIGURE 4 (A) Contact force-time and (B) energy-time plots of trapezoidal sandwich structure under impact load, (C) deformations in the sandwich structure as a result of impact.

seen to decrease sharply. Here, the upper facesheet structure was damaged and the force was wasted.[43] At this point, it is seen that there is a big difference between experimental and numerical results. In other words, the force drop was higher in the numerical result.

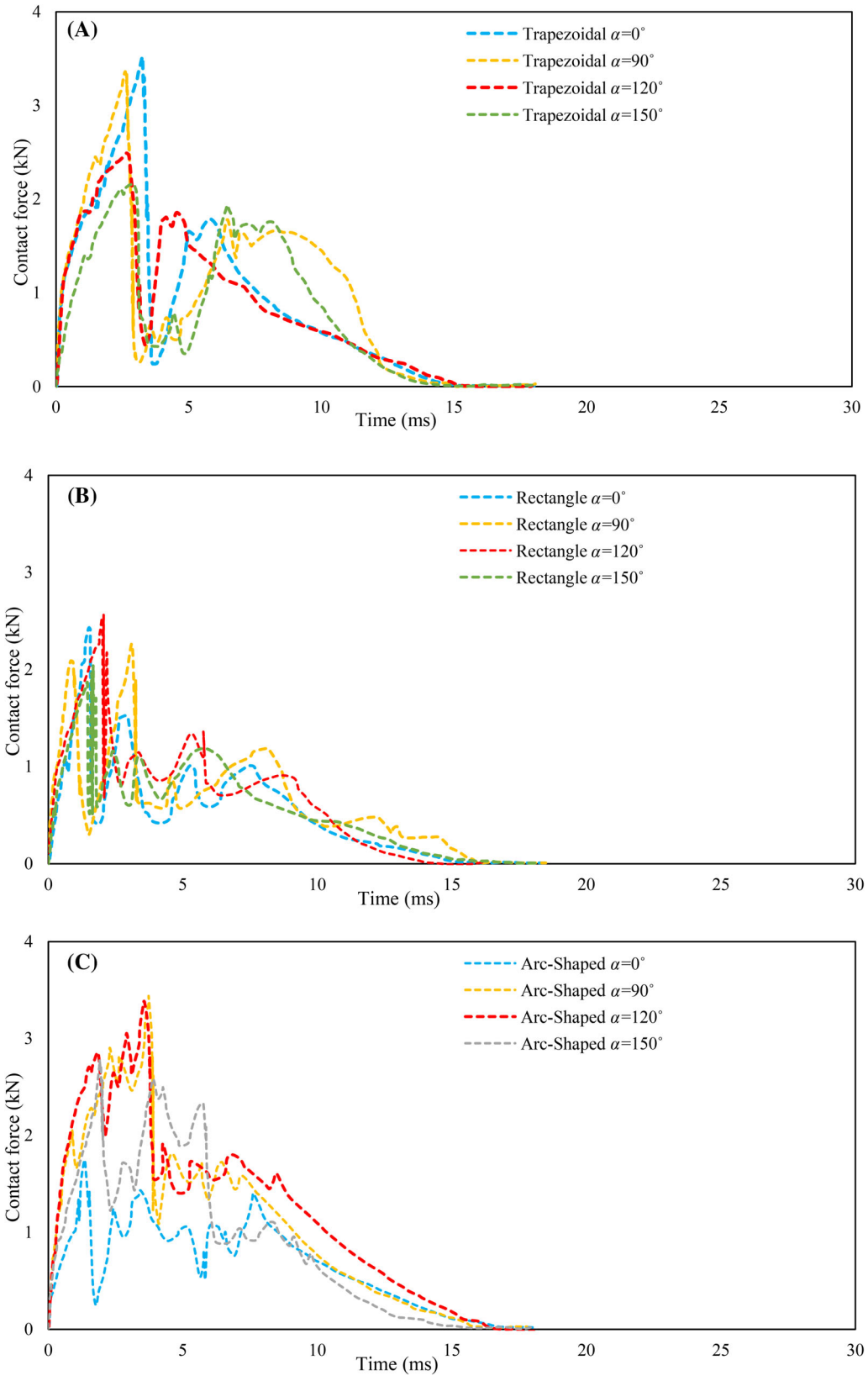

FIGURE 5 Contact force-time graphs for (A) trapezoidal, (B) rectangular, (C) arc-shaped, (D) triangular and (E) sinusoidal core.

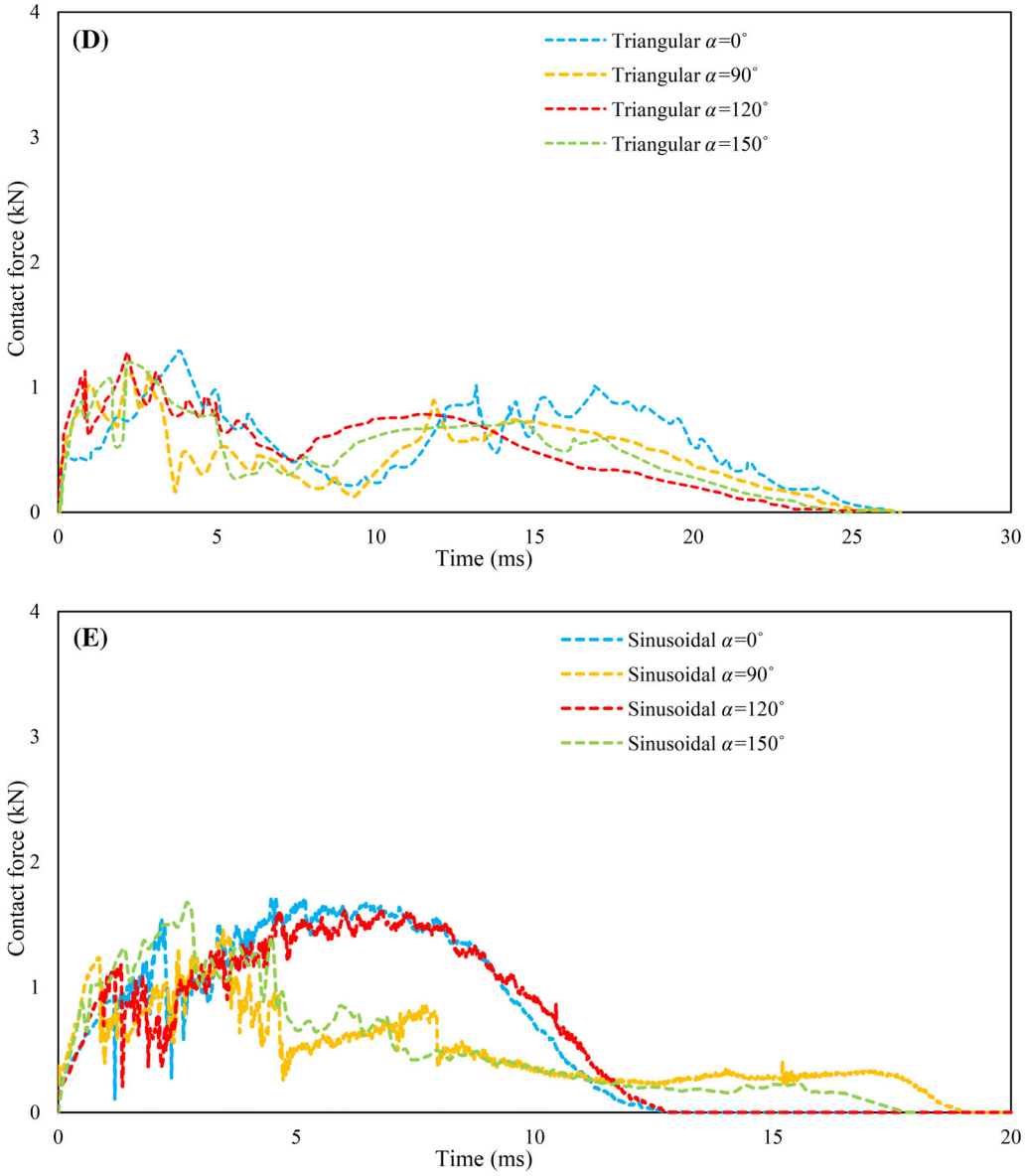

FIGURE 5 (Continued)

The reason for this is that in the FE model, when the stress values on an element reach a certain critical value, the element is erased.[44] Therefore, when the elements in contact with the impactor tip are erased, the force value decreases. But in the experimental study, even if the elements are damaged, they contact the impactor tip and generate a small force.[45] Therefore, due to this force difference, the force drop in the experimental study was less. It is seen that there are oscillations as the force value increases to the peak point. These oscillations are due to the propagation of the force between the elements as it increases and the stress accumulation in the layers.[46] After the force decreased, it increased again. However, the force value did not increase as much as at the first contact moment. Because the stability of the system was weakened.[8] Then, the force value reaching the second peak value decreased and the force value became 0. When the force value is 0, it means that the energy of the impactor runs out and returns and stops contact with the sandwich structure. This is seen in the energy graph in Figure 4B. In Figure 4C, the deformations caused by the impact are given experimentally and numerically. The experimental deformation pictures of the sandwich structures are taken from Ref. [21]. In Figure 4C, the places shown in blue in the FEM represent the undamaged places. The locations shown in red represent the damaged locations. When the experimental study and FEM damage area are compared, it is seen that they are close to each other. In FEM, the elements

at the damaged point were deleted. In the experimental study, it collapsed inward due to pressure. In both experimental and FEM, the damage did not reach the interior. In other words, the entire damage was absorbed by the upper facesheets and core structure. Because the core structure provides support below the point of contact of the impactor. There are points in the core structure where the core structure does not contact or support. If the impact is applied to these points, the amount of damage will be greater because there is no core support.[27] Another important parameter affecting the damage magnitude is the impact energy.[47]

When composite structures are subjected to impact, they try to absorb the impact with damage types such as matrix damage, delamination and fiber fracture. The biggest energy absorbing damage type is matrix damage.[48] When fiber fracture occurs, the damage process is completed in the structure. In materials such as aluminum, this impact reaction is not as complex as in composite

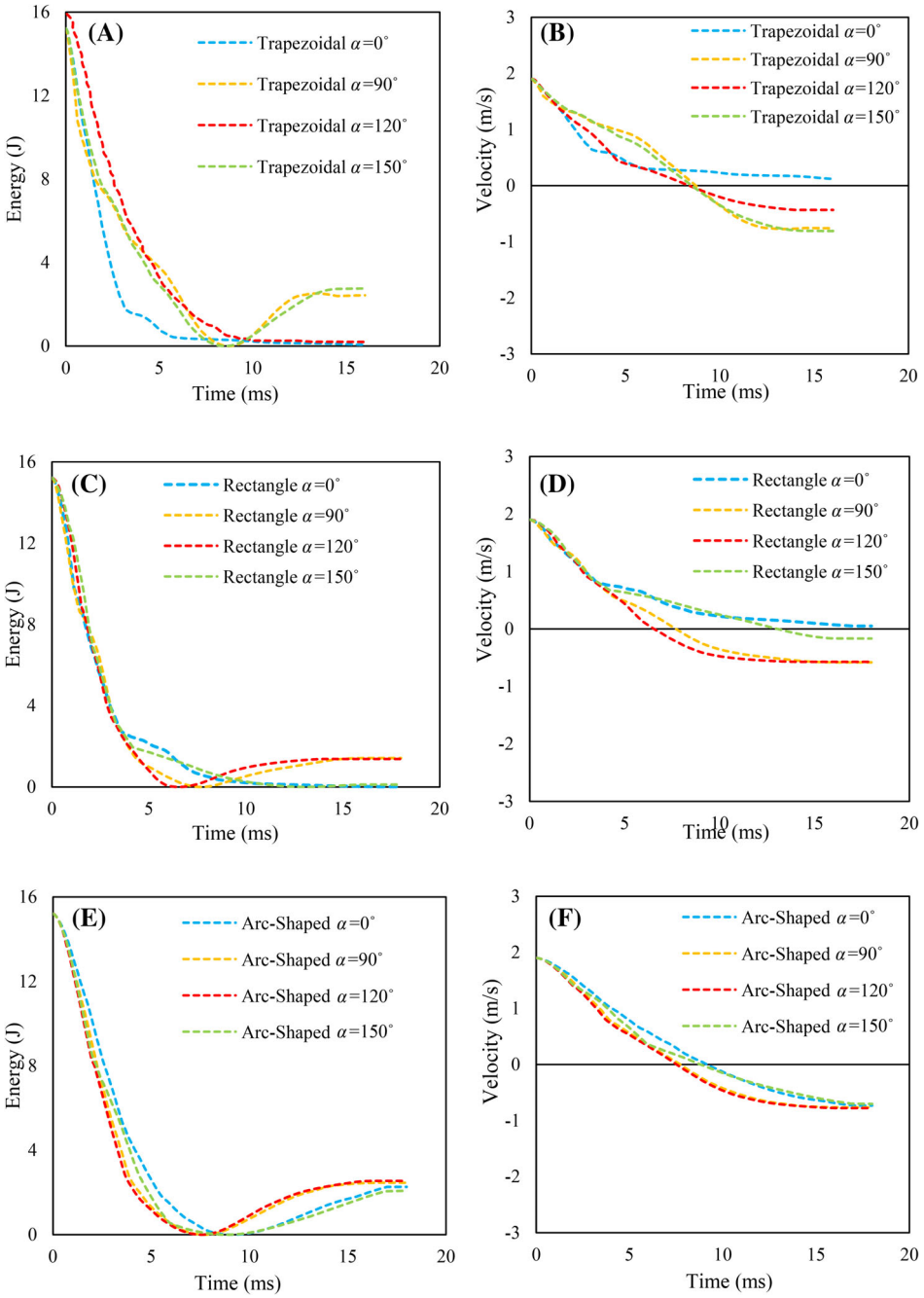

FIGURE 6 Energy-time and velocity-time graphs (A) and (B) for trapezoidal, (C) and (D) for rectangular, (E) and (F) for arc-shaped, (G) and (H) for triangular and (I) and (J) for sinusoidal core.

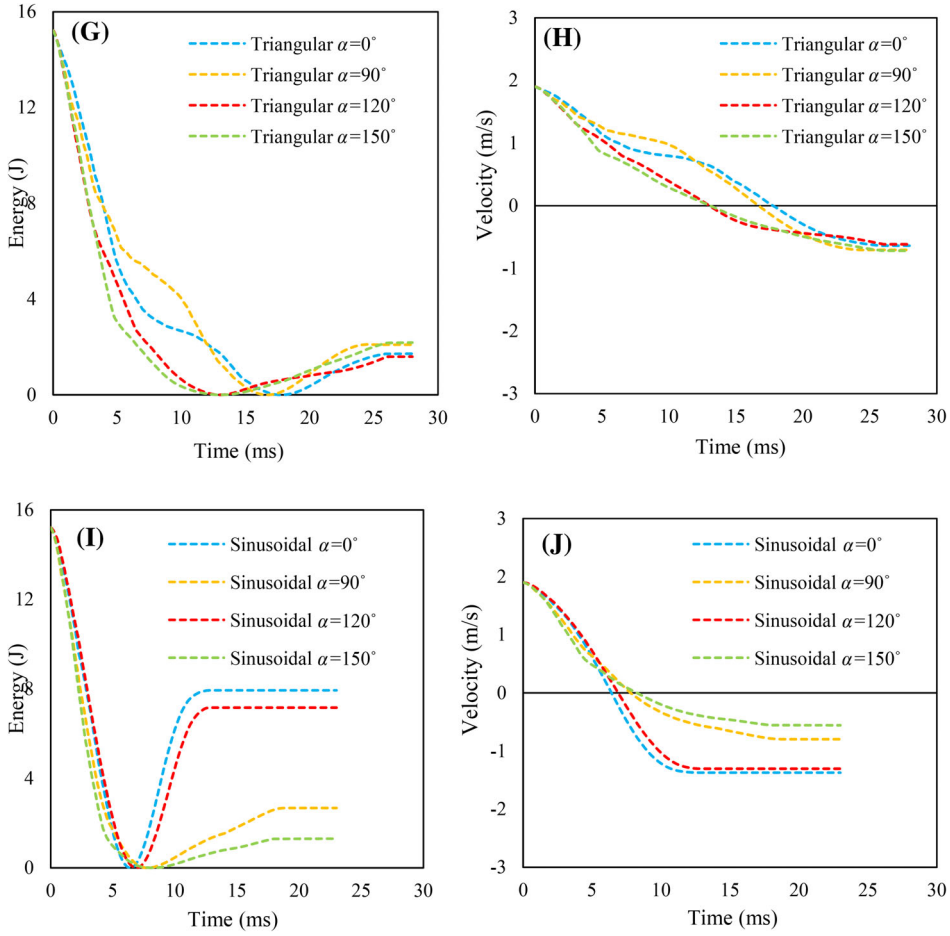

FIGURE 6 (Continued)

structures. Since they have a homogeneous structure, there is liner up to a certain critical value. In composite structures, on the other hand, it is more complex to predict the mechanical behavior under load because there are many different factors. Because there are many factors such as the type of matrix used, fiber thickness, matrix-fiber adhesion compatibility, production temperature, etc. All these factors are important in terms of engineering as they affect the mechanical performance of the structure.

With the numerical model supported by the experimental study, the impact performances of specimens with five different core structures and curve angles were analyzed. The same boundary conditions as the experimental study were used in these analyses. Figure 5 shows the contact force-time graphs for (A) Trapezoidal, (B) Rectangular, (C) Arc-shaped, (D) Triangular and (E) Sinusoidal core sandwich specimen with different curve angles (0°, 90°, 120°, 150°). When the contact force-time graph in Figure 5A is for trapezoidal core examined, the force first reached the maximum point and then decreased sharply for all four angle values. It is seen that the impact reactions are parallel even if the curve angles are different. For the trapezoidal core structure, while the peak force was 3.52 kN at 0°, it decreased to 2.16 kN at 150°. Therefore, the peak force value decreased by 38.6% with the change of curve angle. Figure 5B–E shows the graphs of rectangular, arc-shaped, triangular and sinusoidal core structures respectively.

Figure 6 shows the energy-time and velocity-time graphs (A) and (B) for Trapezoidal, (C) and (D) for Rectangular, (E) and (F) for Arc-shaped, (G) and (H) for Triangular and (I) and (J) for Sinusoidal core structure with different curve angles (0°, 90°, 120°, 150°). When the energy-time graph of Figure 6A is examined, it is seen that the initial energy of the impactor is 15 J. After the impactor contacts the specimen, its energy is 0 and then the impact test ends with a certain energy. Absorbed energy efficiency (η) value should be determined to determine the energy absorption performance of the specimens or sandwich structures with different core structures and to compare them with each other. When calculating this value, the difference between the initial and final energy is divided by the initial energy.

For example, for the sample $\alpha = 90°$, the absorbed energy efficiency (η) value of 0.947 is obtained when the difference between the initial energy (15 J) and the final energy value (0.79 J) is divided by the initial energy. Figure 6B velocity-time graph shows the velocity curves of the impactor. When the graph is examined, it is seen that the

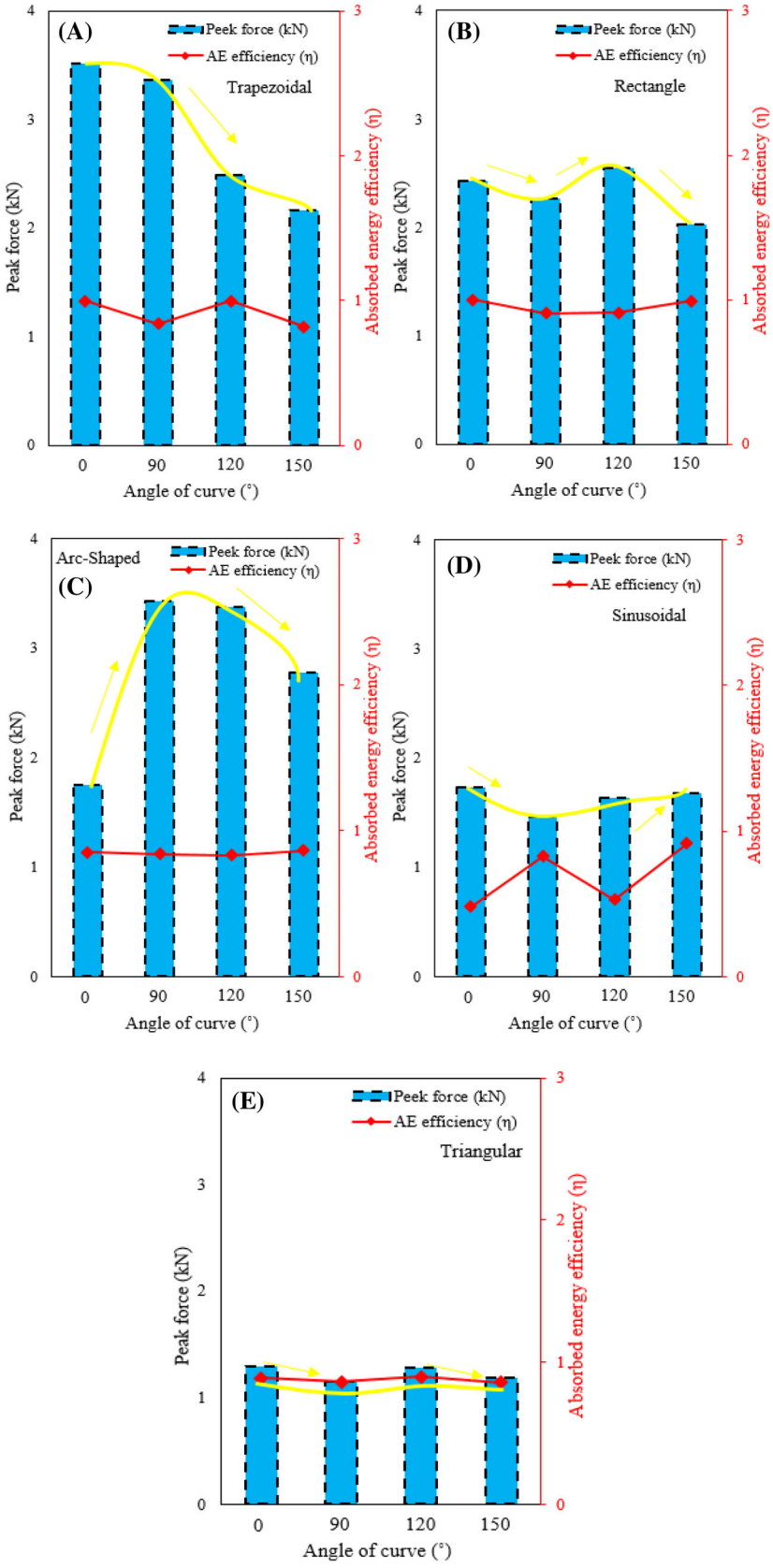

FIGURE 7 Variation of peak force and absorbed energy efficiency in sandwich structures as a result of impact.

impactor velocities change from positive to negative. Here the direction of the impactor is assigned as $+z$. Since the impactor moved in the opposite direction of the z direction, that is, in the $-z$ direction, while returning from the specimen surface, it entered the negative area in the graph. It is seen that the energy graphs are parallel to the velocities. Figure 6C–J shows the graphs of rectangular, arc-shaped, triangular and sinusoidal core structures respectively.

In the Figure 7 contact force and energy absorption efficiency results for (A) Trapezoidal, (B) Rectangular, (C) Arc-shaped, (D) Triangular and (E) Sinusoidal core sandwich specimen with different curve angles (0°, 90°, 120°, 150°). In the Figure 7A when the results for the trapezoidal core sandwich structure are analyzed, the peak force value decreases by 38.6 kN% as the angle α increases (i.e., from 0° to 150°). To show this decrease more clearly, the yellow colored decrease curve has been added. Absorbed energy efficiency value varies according to the angle α. In other words, while the energy efficiency is 0.99 when $\alpha = 0°$, it becomes 0.84, 0.99 and 0.81 when $\alpha = 90°$, 120°, and 150° respectively. Therefore, the energy efficiency of trapezoidal core sandwich structures varies according to the angle. In this study, numerical

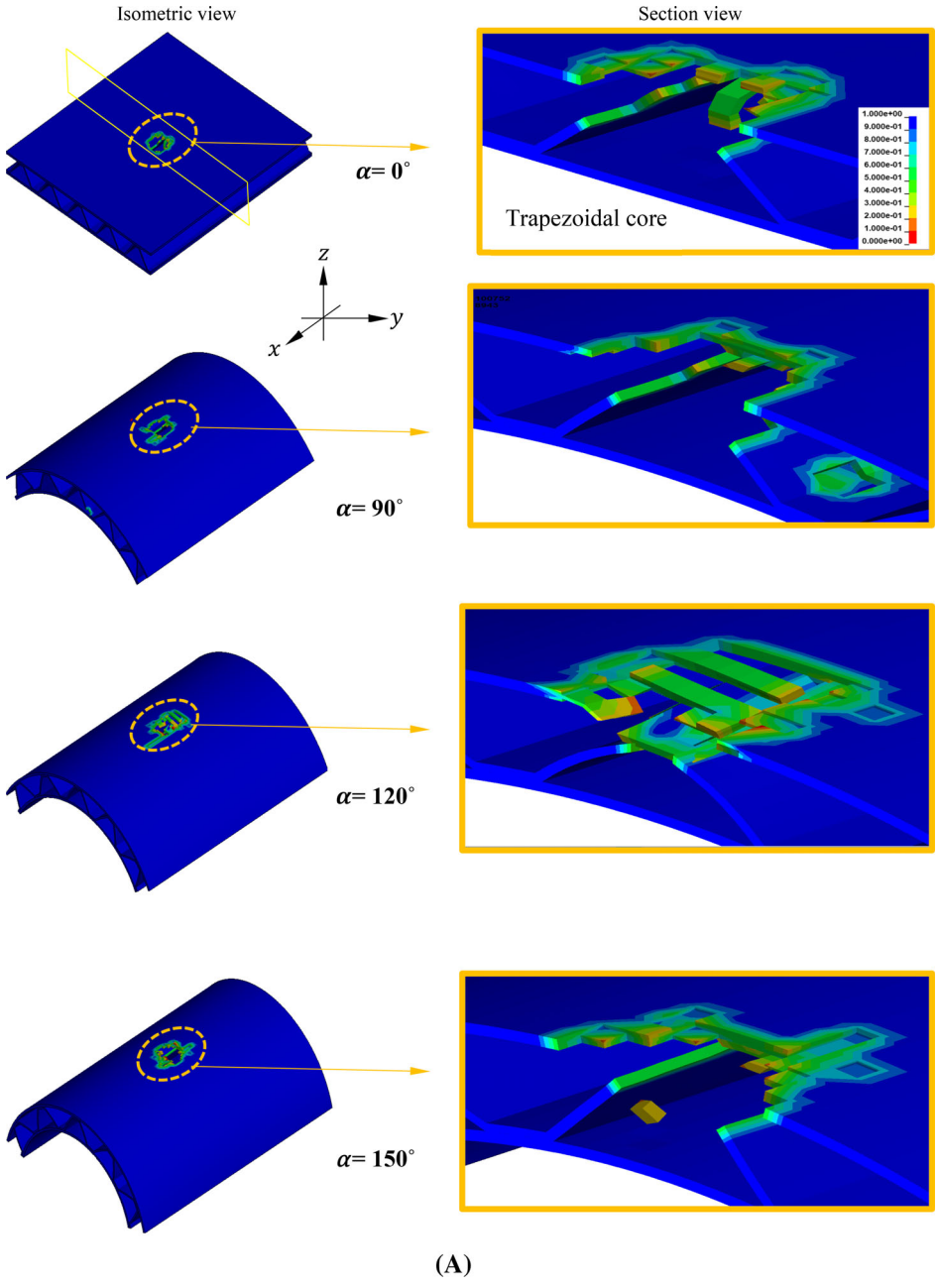

FIGURE 8 Damage to the (A) trapezoidal, (B) rectangular, (C) arc-shaped, (D) triangular and (E) sinusoidal core sandwich structure.

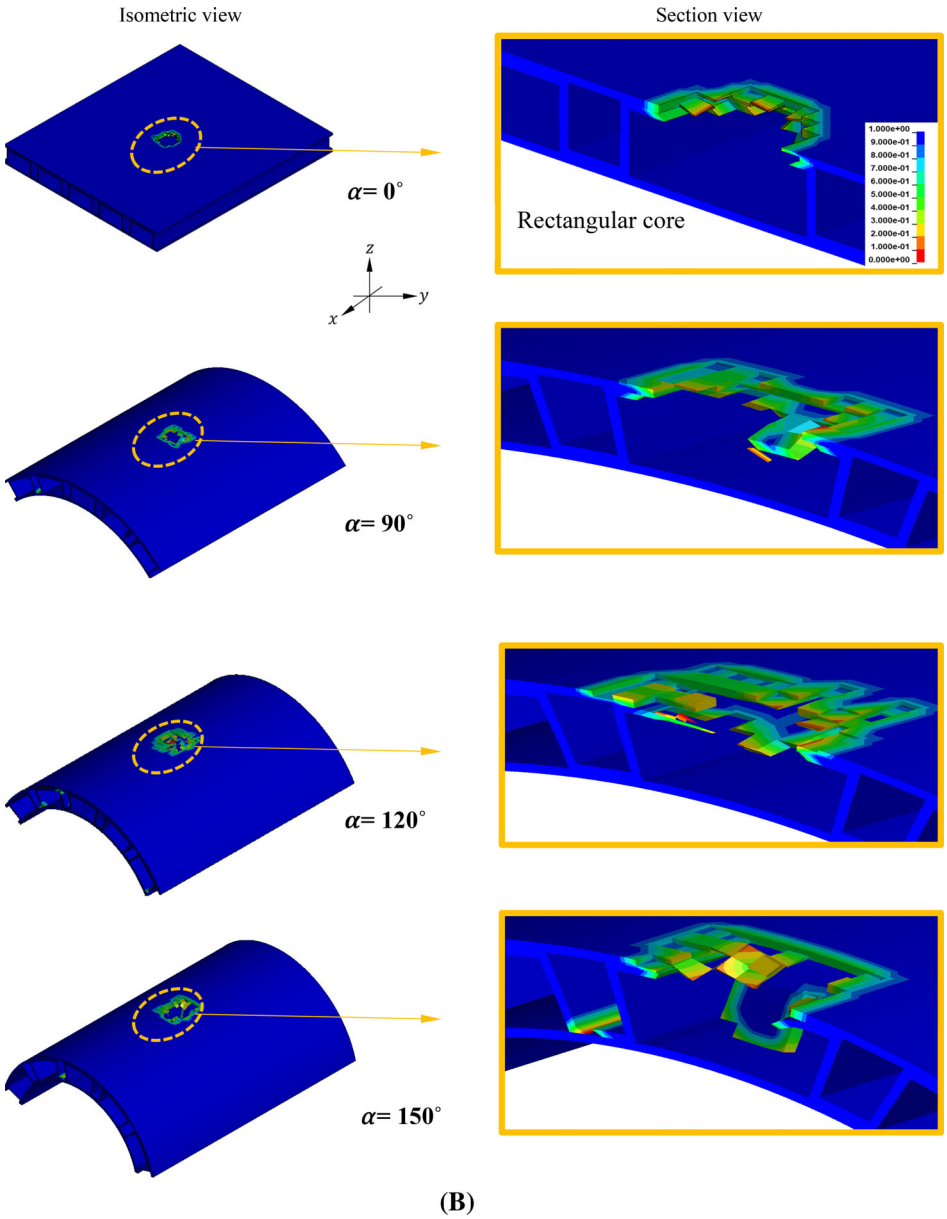

FIGURE 8 (Continued)

simulations were performed for 0°, 90°, 120° and 150° for α only. In order to determine exactly which angle is the turning point, that is, after which angle the energy efficiency changes, the angle increment ratio should be kept low and many numerical simulations should be performed. When the results for the Figure 7B rectangle core sandwich structure are examined, it is seen that as the curve angle increases, the peak force value first decreases, then increases and then decreases again. The highest peak force value is 2.55kN for $\alpha = 120°$. The energy efficiency also started at the highest, then decreased and finally increased again. Figure 7C shows the arc-shaped results. It is seen that the peak force values here have the opposite effect of the Sinusoidal sandwich structure given in Figure 7D. When the absorbed energies are compared, it is seen that the arc-shaped structure has a more stable effect, while the energy efficiency is clearly affected by the change of the curve angle in the Sinusoidal structure. In Figure 7E, when the results for the triangular sandwich structure are analyzed, it is seen that the peak force value is the lowest for the other four different corrugated core structures. The average peak force (i.e. the average peak force for the four different angles) is 1.22 kN. The core structure with the highest peak force average is the Trapezoidal core sandwich structure with 2.88 kN. When absorbed energy efficiency is compared; the highest absorbed energy efficiency average is rectangle with 0.95 and the lowest is sinusoidal core with 0.69.

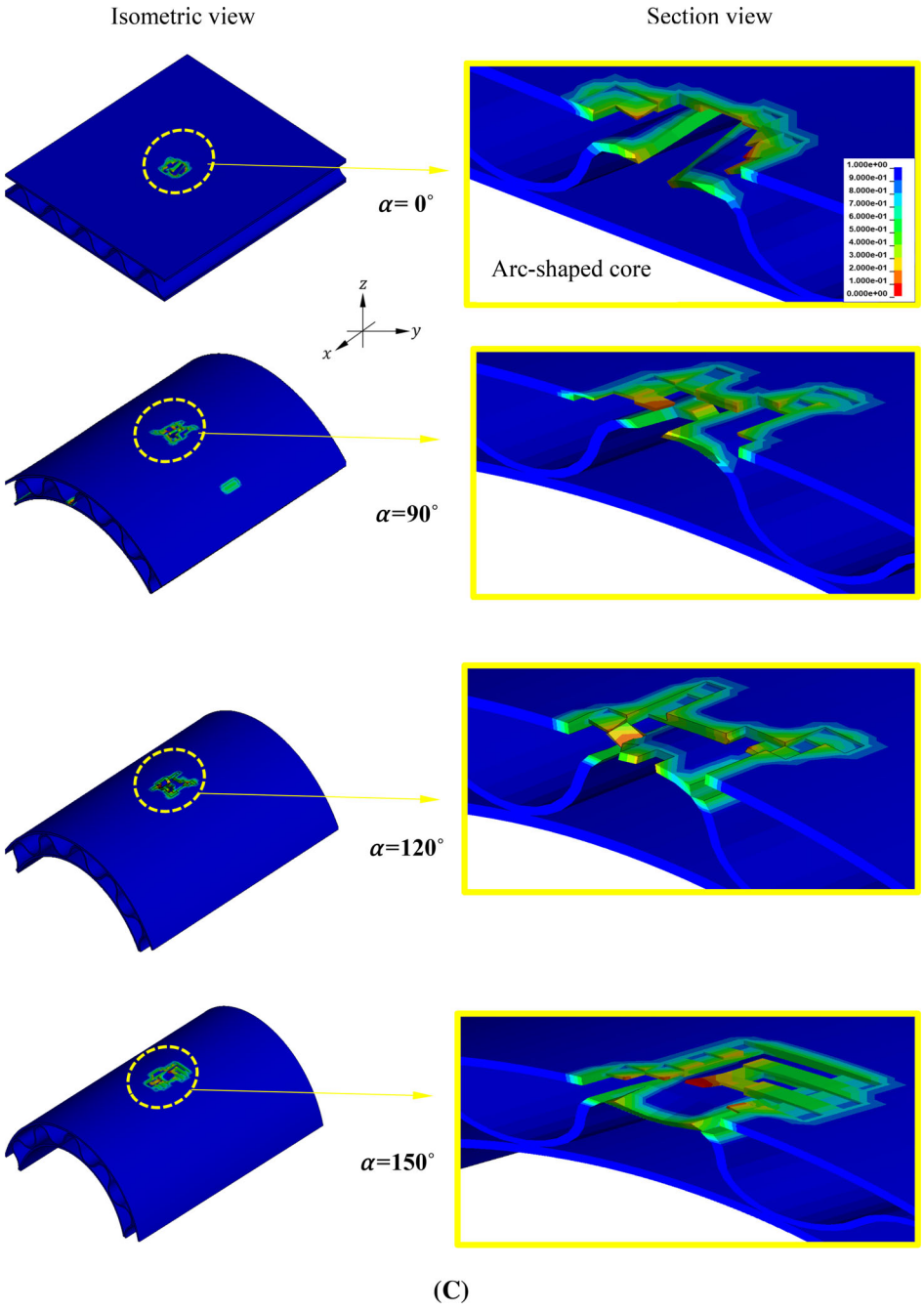

FIGURE 8 (Continued)

Composite structures are used in many sectors and components due to their superior mechanical properties. Therefore, they can be exposed to many loads and impacts according to the type of usage area. When composite structures are subjected to impact, depending on the severity of the impact, it may leave some permanent damage to the structure. These damages are sometimes visible and sometimes occur as delamination damage between layers and are not visible. These damages may grow during use and with the effect of fatigue and may cause sudden major damages and disasters.[49] Therefore, it is important to know the damage behavior of composite structures well. When composite structures are subjected to impact, they absorb this impact by matrix damage, fiber fracture and delamination damage to absorb the impact. With the impact of the incoming impact, damage to the matrix structure occurs first.[50]

Then delamination damage occurs in the layers. The damage process is completed with the occurrence of fracture in the fibers. Figure 8A–E shows the deformations of sandwiches with trapezoidal, rectangular, arc-shaped, triangular and sinusoidal core structures respectively.

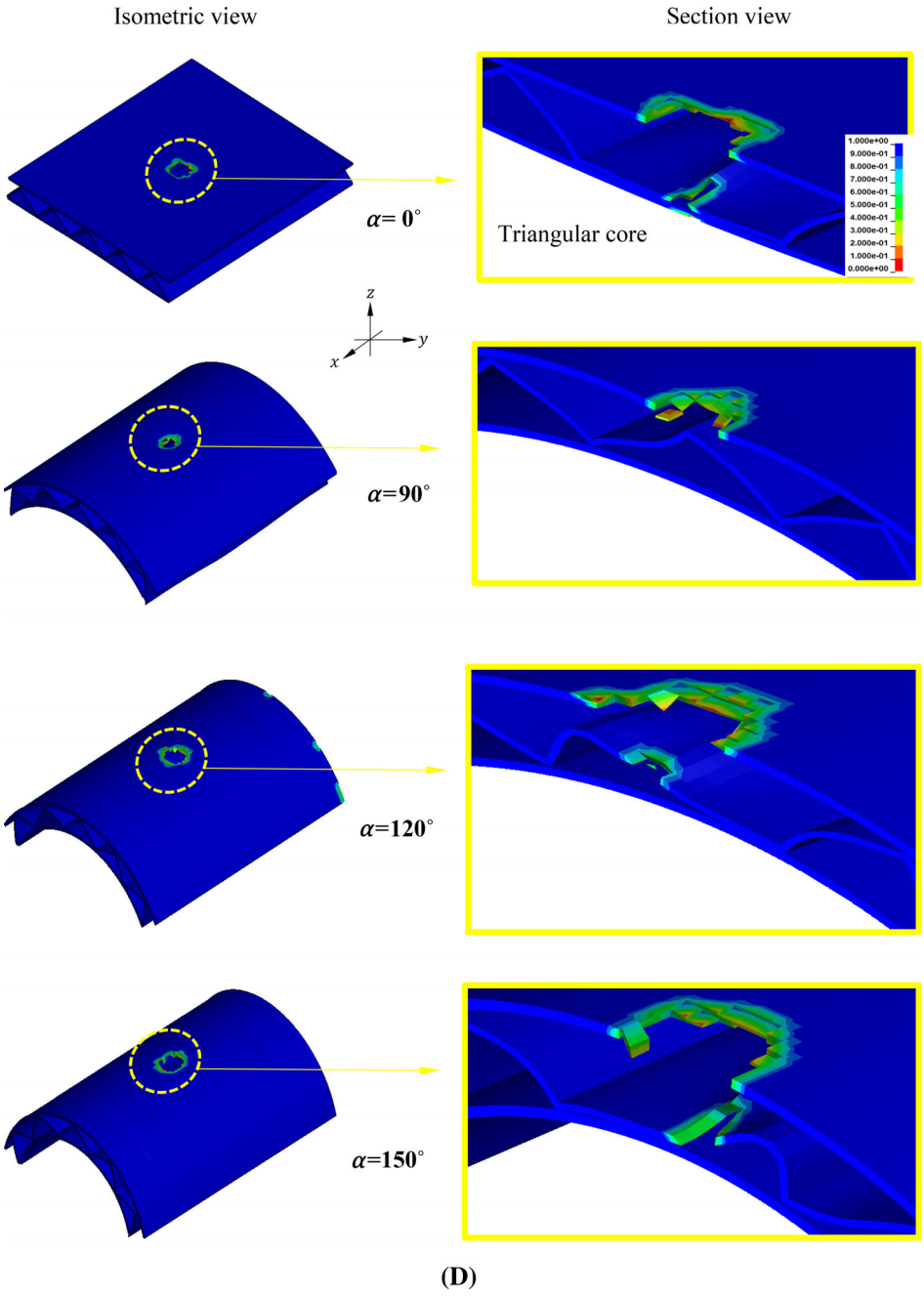

FIGURE 8 (Continued)

For each core structure, isometric and section view are added separately for each curve angle. Cross section in x direction was used for section view of the core structure. In the damage pictures, the elements shown in blue color represent the undamaged elements. The elements shown in red color represent the damaged elements. When all damages are analyzed, it is seen that the biggest damage occurred in the top facesheets structure.[9] No damage occurred in the bottom facesheet for all specimens. Therefore, the top facesheets and core absorbed all the impact energy. It is seen that the damage areas increase with increasing curve angle. In trapezoidal, rectangular and arc-shaped structures, the core structure showed impact resistance and was damaged. In the triangular structure, the core structure changed shape and absorbed the energy.

In addition, since there was no support under the apex of the triangular structure, the peak force value was also the lowest.[51]

Since a real-time impact test occurs very quickly, it is not possible to visually see or follow the damage progression. However, it is possible to see the damage

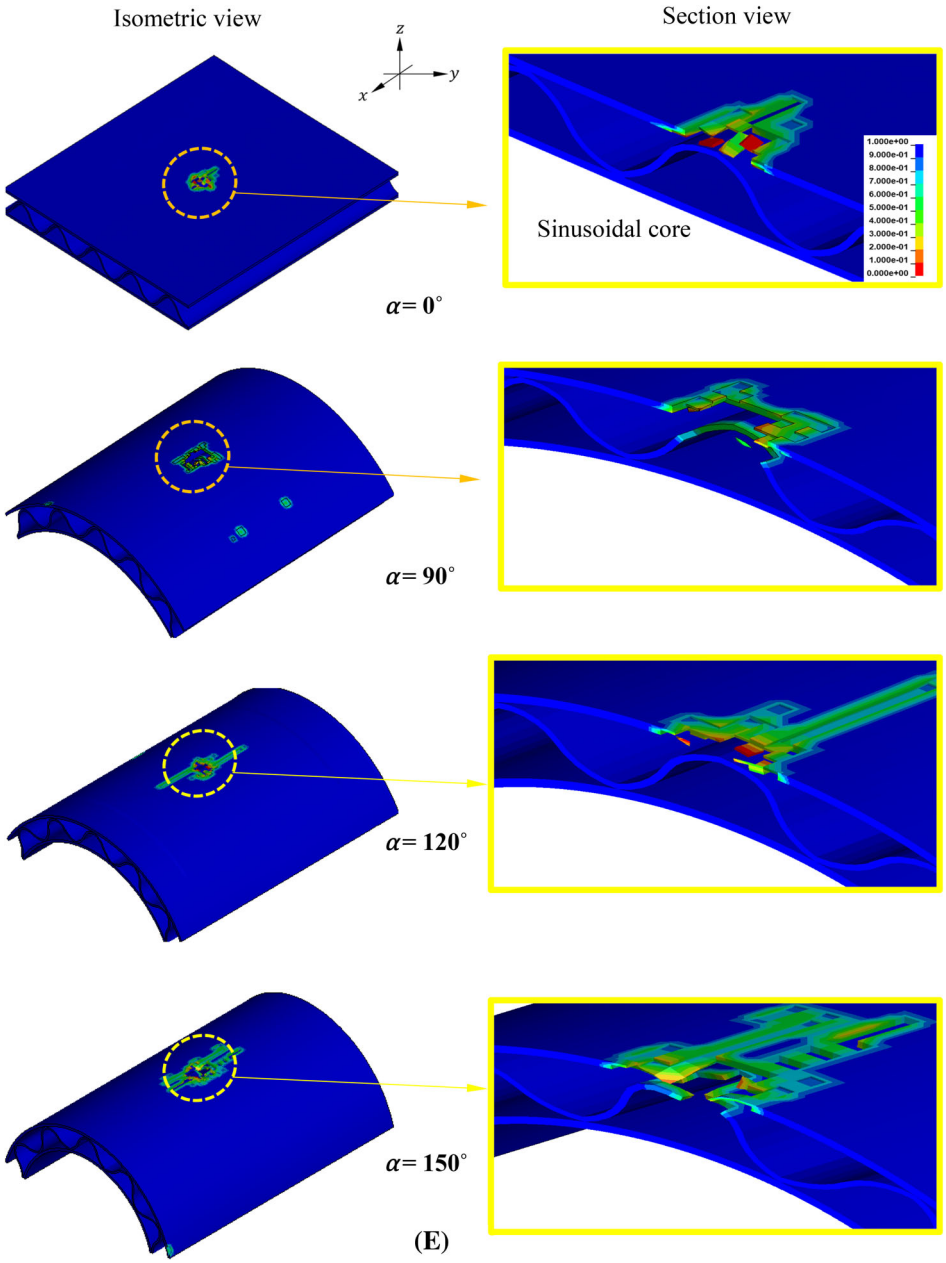

FIGURE 8 (Continued)

progression by slowing down the image with technological cameras. This also requires high cost. Thanks to FE theology, it is possible to see all the damage phases from the beginning to the end of the impact test with all the details.[33] Figure 9 shows the end of contact force-time of arc-shaped and rectangle core sandwich structures with curve angle (α) 120. In the graph, the onset of the first damage, the damage state after the peak force and the final damage state are gradually added. After the impactor contacts the specimen surface, stresses occur in the elements at the point of contact. Damage starts when the stress values at this point reach the critical value threshold of the material due to the impact effect.[52] The first damage onset is 0.8 ms for arc-shaped and 0.52 ms for rectangle. Due to the flexible shape of the arc-shaped structure, the damage started later. Immediately after the contact force reaches its peak, there is a sharp drop in force.

Damage and element deletion occurred in the upper facesheet structures. At the end of the impact simulation, matrix damages occurred in the top facesheets and core for both specimen structures. It is seen that the damage area in the rectangle structure is higher than the arc-shaped structure. Because the energy absorption efficiency is higher.

Impact simulations were performed for a total of 20 different specimens, including five different core

structures used in this study and four different curve angles for each core structure. Specific energy absorption (SEA) values were calculated and compared in Figure 10. SEA is calculated by dividing the energy absorbed by the specimen by the core mass.[27] In addition, the SEA values of sandwich structures in the literature[9,53–55] were calculated and added to the graph. Triangular core has the highest SEA value with 0.312 J/g close to the other structures because it is lighter even though its energy absorption value is close to the other samples. Sinusoidal core has the smallest SEA value with 0.178 J/g. The SEA value of the Triangular core structure with a curve angle of 0° is 3.4% lower than Ozen et al,[50] 6.3% higher than Yalkin et al[55] and 25.6% higher than Damghani et al[53] The important point here is the type of performance required by the sector or component where sandwich structures will be used. SEA value is very important in the aviation sector where light weight is important. However, in the vehicle industry where energy absorption during impact is very important, the appropriate core structure should be selected by considering energy absorption efficiency.

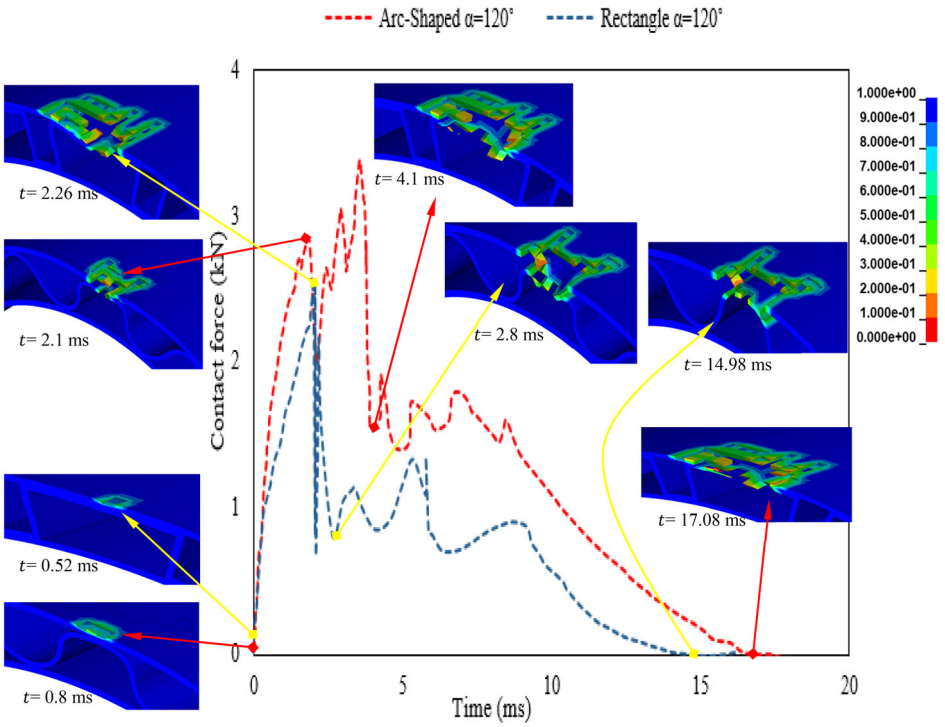

FIGURE 9 Damage images of the arc-shaped and rectangle core sandwich specimens.

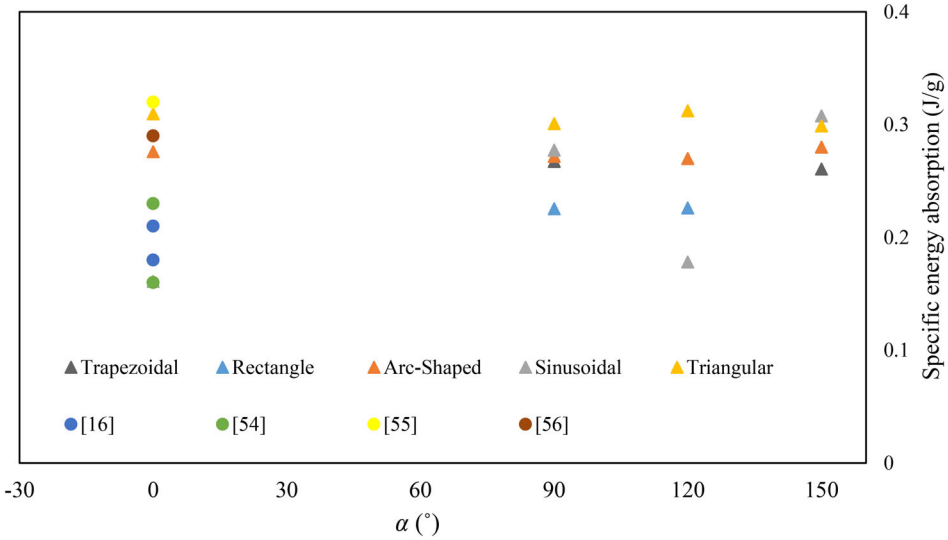

FIGURE 10 Comparison of SEA values.

5 | CONCLUSIONS

In this study, the low-velocity impact behavior of five different carbon fiber reinforced orthogonal woven fabric composite sandwich structures with different geometric configurations and curve angles were numerically investigated. Low-velocity impact tests were performed in *LS DYNA* finite element program to investigate the effects of core type and curve angle on maximum contact force, energy absorption efficiency, specific absorbed energy and failure mode. The results of the study can be summarized as follows;

In the trapezoidal core sandwich structure, the peak force value decreased by 38.6 kN % as the angle α increased (from 0° to 150°). In other structures, the load change was not linear with the curve angle change. Among the five different cores, the peak force average was the highest for the trapezoidal core with 2.9 kN and the lowest for the triangular core sandwich structure with 1.23 kN.

Absorbed energy efficiency average was highest for rectangular core with 0.95 and lowest for sinusoidal core with 0.69.The specific absorbed energy value was highest in triangular core with 0.312 J/g and lowest in sinusoidal core with 0.178 J/g. As the curve angle increased, the damage area on the structure also increased. It was determined that core structure and curve angle is an effective parameter on peak force and energy absorption efficiency.

DATA AVAILABILITY STATEMENT

The data that support the findings of this study are available from the corresponding author upon reasonable request.

ORCID

Ilyas Bozkurt https://orcid.org/0000-0001-7850-2308

REFERENCES

1. Erdem S, Kaman MO. Pin loading effect on 3D spacer fabric-laminated composites produced vacuum infusion. *J Compos Mater*. 2022;56(1):3-16. doi:10.1177/00219983211018265
2. Albayrak M, Kaman MO. Production of curved surface composites reinforced with rubber layer. *Eur J Technic*. 2021;11(1):19-22. doi:10.36222/ejt.824761
3. Kaman MO, Solmaz MY, Turan K. Experimental and numerical analysis of critical buckling load of honeycomb sandwich panels. *J Compos Mater*. 2010;44(24):2819-2831. doi:10.1177/0021998310371541
4. Albayrak M, Kaman MO, Bozkurt I. Experimental and numerical investigation of the geometrical effect on low velocity impact behavior for curved composites with a rubber interlayer. *Appl Compos Mater*. 2023;30(2):507-538. doi:10.1007/s10443-022-10094-5
5. Hajjari M, Jafari Nedoushan R, Dastan T, Sheikhzadeh M, Yu WR. Lightweight weft-knitted tubular lattice composite for energy absorption applications: an experimental and numerical study. *Int J Solids Struct*. 2021;213:77-92. doi:10.1016/j.ijsolstr.2020.12.017
6. Odacı İK. (TEZ) experimental and numerical evaluation of the blast-like loading of fiber reinforced polymer composites and aluminum corrugated Core composite sandwiches through projectile impact testing using aluminum corrugated projectiles, September. 27 2015.
7. He W, Liu J, Tao B, Xie D, Liu J, Zhang M. Experimental and numerical research on the low velocity impact behavior of hybrid corrugated core sandwich structures. *Compos Struct*. 2016;158:30-43. doi:10.1016/j.compstruct.2016.09.009
8. Liu J, He W, Xie D, Tao B. The effect of impactor shape on the low-velocity impact behavior of hybrid corrugated core sandwich structures. *Compos Part B Eng*. 2017;111:315-331. doi:10.1016/j.compositesb.2016.11.060
9. He W, Liu J, Wang S, Xie D. Low-velocity impact response and post-impact flexural behaviour of composite sandwich structures with corrugated cores. *Compos Struct*. 2018;189(January):37-53. doi:10.1016/j.compstruct.2018.01.024
10. Zhang Q, Fang H, Zhu L, et al. Impact behavior of corrugated-core infilling foam sandwich composite structure. *Case Stud Construct Mater*. 2022;17:e01418. doi:10.1016/J.CSCM.2022.E01418
11. Hou S, Zhao S, Ren L, Han X, Li Q. Crashworthiness optimization of corrugated sandwich panels. *Mater Des*. 2013;51:1071-1084. doi:10.1016/j.matdes.2013.04.086
12. Ge L, Zheng H, Li H, Liu B, Su H, Fang D. Compression behavior of a novel sandwich structure with bi-directional corrugated core. *Thin-Walled Struct*. 2021;161:107413. doi:10.1016/J.TWS.2020.107413
13. Cao BT, Hou B, Li YL, Zhao H. An experimental study on the impact behavior of multilayer sandwich with corrugated cores. *Int J Solids Struct*. 2017;109:33-45. doi:10.1016/J.IJSOLSTR.2017.01.005
14. Kiliçaslan C, Güden M, Odaci IK, Taşdemirci A. The impact responses and the finite element modeling of layered trapezoidal corrugated aluminum core and aluminum sheet interlayer sandwich structures. *Mater Des (1980–2015)*. 2013;46:121-133. doi:10.1016/J.MATDES.2012.09.059
15. Yu Z, Liu K, Zhou X, Jing L. Low-velocity impact response of aluminum alloy corrugated sandwich beams used for high-speed trains. *Thin-Walled Struct*. 2023;183:110375. doi:10.1016/J.TWS.2022.110375
16. Li Z, Yang Q, Chen W, et al. Impact response of a novel sandwich structure with Kirigami modified corrugated core. *Int J Impact Eng*. 2021;156:103953. doi:10.1016/J.IJIMPENG.2021.103953
17. Acanfora V, Sellitto A, Russo A, Zarrelli M, Riccio A. Experimental investigation on 3D printed lightweight sandwich structures for energy absorption aerospace applications. *Aerosp Sci Technol*. 2023;137:108276. doi:10.1016/J.AST.2023.108276
18. Garofano A, Acanfora V, Riccio A. On the use of hybrid shock absorbers to increase safety of commercial aircraft passengers during a crash event. *Prog Aerosp Sci*. 2024;148:101004. doi:10.1016/J.PAEROSCI.2024.101004

19. Rong Y, Liu J, Luo W, He W. Effects of geometric configurations of corrugated cores on the local impact and planar compression of sandwich panels. *Compos Part B Eng*. 2018;152(August):324-335. doi:10.1016/j.compositesb.2018.08.130
20. Zhao T, Jiang Y, Zhu Y, et al. An experimental investigation on low-velocity impact response of a novel corrugated sandwiched composite structure. *Compos Struct*. 2020;252, no. June:112676. doi:10.1016/j.compstruct.2020.112676
21. Yang JS, Zhang W-M, Yang F, et al. Low velocity impact behavior of carbon fibre composite curved corrugated sandwich shells. *Compos Struct*. 2020;238(August 2019):1-16. doi:10.1016/j.compstruct.2020.112027
22. Cheng Y, Liu K, Li Y, Wang Z, Wang J. Experimental and numerical simulation of dynamic response of U-type corrugated sandwich panels under low-velocity impact. *Ocean Eng*. 2022;245:110492. doi:10.1016/J.OCEANENG.2021.110492
23. Boonkong T, Shen YO, Guan ZW, Cantwell WJ. The low velocity impact response of curvilinear-core sandwich structures. *Int J Impact Eng*. 2016;93:28-38. doi:10.1016/j.ijimpeng.2016.01.012
24. Yellur MR, Seidlitz H, Kuke F, Wartig K, Tsombanis N. A low velocity impact study on press formed thermoplastic honeycomb sandwich panels. *Compos Struct*. 2019;225(November 2018):111061. doi:10.1016/j.compstruct.2019.111061
25. Susainathan J, Eyma F, DE Luycker E, Cantarel A, Castanie B. Numerical modeling of impact on wood-based sandwich structures. *Mech Adv Mater Struct*. 2020;27(18):1583-1598. doi:10.1080/15376494.2018.1519619
26. Shirbhate PA, Goel MD. Investigation of effect of perforations in honeycomb sandwich structure for enhanced blast load mitigation. *Mech Adv Mater Struct*. 2023;30(17):3463-3478. doi:10.1080/15376494.2022.2076958
27. Bozkurt I, Kaman MO, Albayrak M. Low-velocity impact behaviours of sandwiches manufactured from fully carbon fiber composite for different cell types and compression behaviours for different core types. *Materialpruefung/Mater Test*. 2023;65(9):1349-1372. doi:10.1515/mt-2023-0024
28. Liu W, Wang S, Bu J, Ding X. An analytical model for the progressive failure prediction of reinforced thermoplastic pipes under axial compression. *Polym Compos*. 2021;42(6):3011-3024. doi:10.1002/pc.26035
29. Sebeay TA, Ahmed A. Numerical investigation into GFRP composite pipes under hydrostatic internal pressure. *Polymers (Basel)*. 2023;15(5):1110-1132. doi:10.3390/polym15051110
30. Abdel-Nasser Y, Elhewy AMH, Al-Mallah I. Impact analysis of composite laminate using finite element method. *Ships Offshore Struct*. 2017;12(2):219-226. doi:10.1080/17445302.2015.1131005
31. Zhang H, Zhang L, Liu Z, Qi S, Zhu Y, Zhu P. Numerical analysis of hybrid (bonded/bolted) FRP composite joints: a review. *Compos Struct*. 2021;262:113606. doi:10.1016/J.COMPSTRUCT.2021.113606
32. Rozylo P, Debski H, Kubiak T. A model of low-velocity impact damage of composite plates subjected to compression-after-impact (CAI) testing. *Compos Struct*. 2017;181:158-170. doi:10.1016/J.COMPSTRUCT.2017.08.097
33. Setoodeh AR, Malekzadeh P, Nikbin K. Low velocity impact analysis of laminated composite plates using a 3D elasticity based layerwise FEM. *Mater Des*. 2009;30(9):3795-3801. doi:10.1016/J.MATDES.2009.01.031
34. Khalili SMR, Soroush M, Davar A, Rahmani O. Finite element modeling of low-velocity impact on laminated composite plates and cylindrical shells. *Compos Struct*. 2011;93(5):1363-1375. doi:10.1016/J.COMPSTRUCT.2010.10.003
35. ASTM D695-96: Standard test method for compressive properties of rigid plastics, American society for testing and materials. 1996.
36. B. Standard, NO COPYING WITHOUT BSI PERMISSION EXCEPT AS PERMITTED BY COPYRIGHT LAW Plastics-Determination of Tensile Properties Part 5: Test Conditions for Unidirectional Fibre-Reinforced Plastic Composites Copyright European Committee for Standardization Provided by IHS under License with CEN Not for Resale No Reproduction or Networking Permitted without License from IHS. 2009.
37. Jo H. LS-DYNA Keyword User's Manual Volume II Material Models, Version 971. Livermore Software Technology Corporation; 24. 2017.
38. Murakami S. *Continuum Damage Mechanics: a Continuum Mechanics Approach to the Analysis of Damage and Fracture*.
39. Hashin Z. Failure criteria for unidirectional fiber composites. *J Appl Mech Transact ASME*. 1980;47(2):329-334. doi:10.1115/1.3153664
40. Dogan F, Hadavinia H, Donchev T, Bhonge PS. Delamination of impacted composite structures by cohesive zone interface elements and tiebreak contact. *Cent Eur J Eng*. 2012;2(4):612-626. doi:10.2478/S13531-012-0018-0
41. Bozkurt I, Kaman MO, Albayrak M. Experimental and numerical impact behavior of fully carbon fiber sandwiches for different core types. *J Braz Soc Mech Sci Eng*. 2024;46(5):318. doi:10.1007/s40430-024-04865-3
42. Sevkat E, Liaw B, Delale F. Drop-weight impact response of hybrid composites impacted by impactor of various geometries. *Mater Des*. 2013;52:67-77. doi:10.1016/j.matdes.2013.05.016
43. Kurşun A, Şenel M, Enginsoy HM, Bayraktar E. Effect of impactor shapes on the low velocity impact damage of sandwich composite plate: experimental study and modelling. *Compos Part B Eng*. 2016;86:143-151. doi:10.1016/j.compositesb.2015.09.032
44. Bozkurt İ AM, Kaman MO. LS-DYNA MAT162 finding material inputs and investigation of impact damage in carbon composite plates. XVrI International Research Conference 2022. 2022.
45. He W, Liu J, Wang S, Xie D. Low-velocity impact behavior of X-frame core sandwich structures – experimental and numerical investigation. *Thin-Walled Struct*. 2018;131(July):718-735. doi:10.1016/j.tws.2018.07.042
46. Albayrak M, Kaman MO, Bozkurt I. The effect of lamina configuration on low-velocity impact behaviour for glass fiber/rubber curved composites. *J Compos Mater*. 2023;57(11):1875-1908. doi:10.1177/00219983231164950
47. Akatay A, Bora MÖ, Çoban O, Fidan S, Tuna V. The influence of low velocity repeated impacts on residual compressive properties of honeycomb sandwich structures. *Compos Struct*. 2015;125:425-433. doi:10.1016/j.compstruct.2015.02.057
48. Zhang C, Tan KT. Low-velocity impact response and compression after impact behavior of tubular composite sandwich

structures. *Compos Part B Eng*. 2020;193(January):108026. doi:10.1016/j.compositesb.2020.108026

49. Solmaz MY, Topkaya T. The flexural fatigue behavior of honeycomb sandwich composites following low velocity impacts. *Appl Sci (Switzerland)*. 2020;10(20):1-14. doi:10.3390/app10207262
50. Shu C, Zhao S, Hou S. Crashworthiness analysis of two-layered corrugated sandwich panels under crushing loading. *Thin-Walled Struct*. 2018;133(July):42-51. doi:10.1016/j.tws.2018.09.008
51. Fan HL, Meng FH, Yang W. Sandwich panels with Kagome lattice cores reinforced by carbon fibers. *Compos Struct*. 2007;81(4):533-539. doi:10.1016/j.compstruct.2006.09.011
52. Alshahrani RF, Merah N, Khan SMA, Al-Nassar Y. On the impact-induced damage in glass fiber reinforced epoxy pipes. *Int J Impact Eng*. 2016;97:57-65. doi:10.1016/j.ijimpeng.2016.06.002
53. Nouri Damghani M, Mohammadzadeh Gonabadi A. Numerical study of energy absorption in aluminum foam sandwich panel structures using drop hammer test. *J Sandw Struct Mater*. 2019;21(1):3-18. doi:10.1177/1099636216685315
54. Özen İ, Çava K, Gedikli H, Alver Ü, Aslan M. Low-energy impact response of composite sandwich panels with thermoplastic honeycomb and reentrant cores. *Thin-Walled Struct*. 2020;156(August):106989. doi:10.1016/j.tws.2020.106989
55. Yalkın HE, Karakuzu R, Alpyıldız T. Low-velocity impact behaviors of sandwich composites with different structural configurations of foam core: numerical study and experimental validation. *Phys Scr*. 2023;98(11):115942. doi:10.1088/1402-4896/ad008f

How to cite this article: Bozkurt I. Effect of geometric configurations and curvature angle of corrugated sandwich structures on impact behavior. *Polym Compos*. 2024;1-24. doi:10.1002/pc.29064